Pain persists in mice lacking both Substance P and CGRPα signaling

Donald Iain MacDonald[1], Monessha Jayabalan[1], Jonathan Seaman[1], Rakshita Balaji[1], Alec Nickolls[1] and Alexander Chesler[1,2*]

[1]*National Center for Complementary and Integrative Health, National Institutes of Health, Bethesda, United States*

[2]*National Institute of Neurological Disorders and Stroke, National Institutes of Health, Bethesda, United States*

*Correspondence: alexander.chesler@nih.gov

Keywords: neuropeptides, Substance P, CGRP, nociception, chronic pain, neuropathic pain, inflammatory pain

Summary

The neuropeptides Substance P and CGRPα have long been thought important for pain sensation. Both peptides and their receptors are expressed at high levels in pain-responsive neurons from the periphery to the brain making them attractive therapeutic targets. However, drugs targeting these pathways individually did not relieve pain in clinical trials. Since Substance P and CGRPα are extensively co-expressed we hypothesized that their simultaneous inhibition would be required for effective analgesia. We therefore generated *Tac1* and *Calca* double knockout (DKO) mice and assessed their behavior using a wide range of pain-relevant assays. As expected, Substance P and CGRPα peptides were undetectable throughout the nervous system of DKO mice. To our surprise, these animals displayed largely intact responses to mechanical, thermal, chemical, and visceral pain stimuli, as well as itch. Moreover, chronic inflammatory pain and neurogenic inflammation were unaffected by loss of the two peptides. Finally, neuropathic pain evoked by nerve injury or chemotherapy treatment was also preserved in peptide-deficient mice. Thus, our results demonstrate that even in combination, Substance P and CGRPα are not required for the transmission of acute and chronic pain.

1. Introduction

Over a hundred neuropeptides are expressed by mammalian neurons (Russo, 2017). Neuropeptides are released through the secretory pathway and activate G-protein coupled receptors to control neuronal excitability and synaptic strength (Pagani et al., 2019). They can also influence the function of immune cells in peripheral tissues (Chiu et al., 2012). Drugs acting on neuropeptides or their receptors are now widely used in the clinic, including therapeutics for obesity and migraine (Drucker, 2022; Ogunlaja and Goadsby, 2022). Which peptides can be targeted successfully and for what indications thus remain key questions for neuroscience and drug development.

Among the most challenging diseases to treat is chronic pain. With over 20% of the population suffering from chronic pain, we urgently need to find new analgesic targets (Nahin et al., 2023). The two neuropeptides most strongly implicated in chronic pain are Substance P and CGRPα (De Matteis et al., 2020; Paige et al., 2022; Yaksh et al., 1980; Zieglgänsberger, 2019). Substance P is an 11-amino acid peptide first discovered as a tissue extract with contractile activity (von Euler and Gaddum, 1931). CGRPα is a 37-amino acid peptide and potent vasodilator identified as the alternatively spliced product of the calcitonin gene (Amara et al., 1982). Both Substance P and CGRPα are highly expressed in pain-responsive neurons throughout the nervous system. In the periphery, strong activation of nociceptor sensory neurons is reported to cause peptide secretion and neurogenic inflammation (Chiu et al., 2012). Similarly, release of Substance P and CGRPα in the spinal cord and brainstem may alter pain transmission in ascending pain pathways (Huang et al., 2019; Latremoliere and Woolf, 2009; Löken et al., 2021). In the brain, these molecules are prominently enriched in areas known to be involved in pain, including the periaqueductal grey, parabrachial nucleus and amygdala (Barik et al., 2018; Lein et al., 2007; Palmiter, 2018). Thus, decades of research implicate Substance P and CGRPα as critical drivers of pain, including modulating tissue inflammation, sensory hypersensitivity, pain chronification and unpleasantness (Chiu et al., 2012; De Matteis et al., 2020; Zieglgänsberger, 2019).

However, selective antagonists of the Substance P receptor NKR1 failed to relieve chronic pain in human clinical trials (Hill, 2000). Although CGRP monoclonal antibodies and receptor blockers have proven effective for subsets of migraine patients, their usefulness for other types of pain in humans is unclear (De Matteis et al., 2020; Jin et al., 2018). In line with this, knockout mice deficient in Substance P, CGRPα or their receptors have been reported to display some pain deficits,

but the analgesic effects are neither large nor consistent between studies (Cao et al., 1998; De Felipe et al., 1998; Guo et al., 2012; Salmon et al., 2001, 1999; Zimmer et al., 1998).

By contrast, ablating or inhibiting peptidergic nociceptors causes profound decreases in heat sensitivity, inflammatory heat hyperalgesia, and some forms of mechanical allodynia (Cowie et al., 2018; McCoy et al., 2013). Mice with silenced Substance P or CGRPα-expressing neurons in brain areas such as the parabrachial nucleus also show impaired pain behavior (Barik et al., 2018; Han et al., 2015; Kang et al., 2022; Sun et al., 2020). In the periphery, Substance P and CGRPα are expressed by largely the same nociceptors, in mice and in humans (Nguyen et al., 2021; Sharma et al., 2020). The two peptides are also co-expressed in the brain (Pauli et al., 2022; Zeisel et al., 2018). Redundancy is built into pain pathways because of their importance for survival and may explain why attenuating the signaling of a single peptide does not recapitulate the analgesic effect of silencing the cell secreting it (Vandewauw et al., 2018).

Given the well-described roles for peptidergic neurons in pain and the widespread co-expression of Substance P and CGRPα, we reasoned that removal of both peptides should reveal roles for peptidergic signaling that might be masked by redundancy. We therefore generated and characterized *Tac1::Calca* double knockout (DKO) mice lacking both Substance P and CGRPα peptides. We predicted these DKO animals might recapitulate the striking absence of inflammatory pain observed in naked mole rats that release glutamate but not Substance P or CGRPα from nociceptors (Park et al., 2008, 2003). Here we present a thorough evaluation of the impact of dual peptide deletion on acute and chronic pain behavior in laboratory mice.

2. Results

2.1. Double knockout mice completely lack Substance P and CGRPα signaling

To investigate the roles of Substance P and CGRPα in pain processing, we generated Tac1::Calca Double Knockout (DKO) mice with constitutive deletion of the two peptide precursor genes. A homozygous Tac1-RFP knockin-knockout line was used to remove the *Tac1* gene encoding preprotachykinin, the precursor for Substance P and Neurokinin A (Wu et al., 2018). As expected, no detectable Substance P immunostaining was observed in pain-relevant areas including the dorsal root ganglion, dorsal horn of the spinal cord, parabrachial nucleus and periaqueductal gray (Figure 1A). To eliminate CGRPα signaling, we used a Calca-Cre mouse, which at homozygosity is a knockout for the *Calca* gene encoding the Calcitonin and CGRPα peptides (Carter et al., 2013; Chen et al., 2018). We were unable to detect CGRP immunoreactivity in DRG, spinal cord and the amygdala (Figure 1B) validating the DKO approach.

A clear prediction from the loss of immunostaining is that sensory neuron activity should no longer activate the neuropeptide receptors. We began by developing a cell-based assay to monitor signaling through the Substance P receptor (NKR1) by generating HEK293 cells stably expressing NKR1, GCaMP6s and Gα15 (so-called 'Substance P-sniffer' cells) (Figure 1C). These cells responded to low nanomolar concentrations of Substance P (EC_{50}=21 nM, Figure 1 – figure supplement 1A), but were insensitive to CGRPα. We reasoned that in co-cultures with DRG neurons, application of the potent TRPV1 agonist capsaicin (10 μM) would stimulate nociceptors to release Substance P and thereby activate neighboring Substance P-sniffer cells. Control DRGs treated with capsaicin evoked robust GCaMP responses in surrounding Substance P-sniffer cells (Figure 1D-E). In contrast, capsaicin stimulated DKO-DRG neurons induced no Substance P-sniffer cell responses (Figure 1D-E).

We also developed a cell-based approach to monitor CGRP release from nociceptors. The CGRP receptor consists of two co-receptors encoded by the genes *Calcrl* and *Ramp1*. We therefore engineered a stable inducible HEK293 sniffer cell line that expressed Calcrl, Ramp1, GCaMP6s and Gα15. These cells responded to low nanomolar concentrations of CGRPα (EC_{50}=27 nM, Figure 1 – figure supplement 1B), but were insensitive to Substance P. When we cultured WT DRG neurons

with the CGRP-sniffer cells, we observed strong increases in calcium consistent with CGRP receptor activity in response to capsaicin application (Figure 1F-H). However, DKO neurons evoked markedly reduced activity in the adjacent sniffer cells (Figure 1D-E). Thus, *Calca* deletion largely abolished endogenous CGRPα signaling. In combination, these experiments demonstrate that deletion of *Tac1* and *Calca* completely blocks the endogenous activation of Substance P and CGRP receptors by nociceptor neurons.

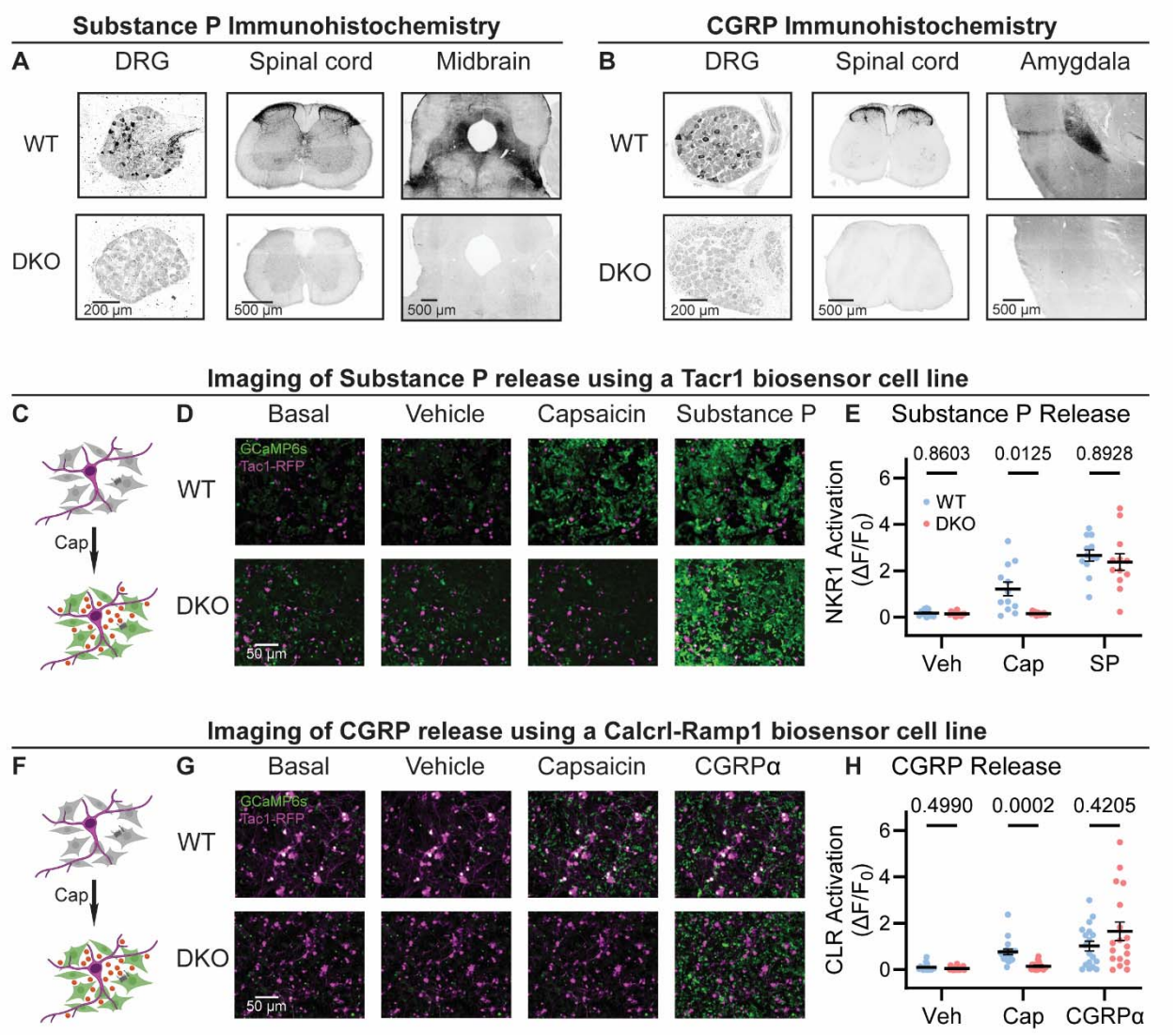

Figure 1. Tac1::Calca DKO mice lack Substance P and CGRPα peptides throughout the nervous system. (A) Confocal images showing Substance P immunostaining in the dorsal root ganglion (DRG), spinal cord dorsal horn and midbrain of a WT mouse (*top*). No staining is detectable in the DKO (*bottom*). **(B)** Confocal images showing CGRP immunostaining in the DRG, spinal cord dorsal horn, and amygdala of a WT mouse (*top*). The DKO mice show no obvious staining (*bottom*). Images in both (A) and (B) are representative of staining performed on tissue from 1M and 1F animal per genotype. **(C)** Schematic showing co-culture of Tac1-RFP-labelled DRG neurons and Substance P-sniffer HEK293 cells expressing NKR1, GCaMP6s and Gαo. Capsaicin-evoked secretion of Substance P from DRG activates the NKR1 receptor in neighboring HEK leading to calcium release from stores and GCaMP6s-mediated fluorescence increase. **(D)** Fluorescence images showing Tac1-RFP-labelled DRG neurons (*magenta*) and Substance P-sniffer cells (*green*). Capsaicin causes an increase in Substance P-sniffer GCaMP6s fluorescence when cultured with DRGs from WT, but not DKO, mice. Application of exogenous Substance P (10 nM) activates Substance P-sniffers in both conditions. **(E)** Quantification of fluorescence change in Substance P-sniffer cells in response to vehicle, capsaicin and Substance P stimulation in WT and DKO mice. n=12 wells from 2 mice (1M, 1F) for WT, and n=12 wells from 2 mice (1M, 1F) for DKO. For (E), means were compared using repeated measures 2-way ANOVA, followed by post-hoc Sidak's test. Error bars denote standard error of the mean. **(F)** Schematic showing co-culture of Tac1-RFP-labelled DRG neurons and Substance P-sniffer HEK293 cells expressing Calcrl, Ramp1, GCaMP6s and Gαo. Capsaicin-evoked secretion of CGRPα from DRG

activates the CGRP receptor complex in neighboring HEK leading to calcium release from stores and GCaMP6s-mediated fluorescence increase. **(G)** Fluorescence images showing Tac1-RFP-labelled DRG neurons (*magenta*) and Substance P-sniffer cells (*green*). Capsaicin causes an increase in CGRP-sniffer GCaMP6s fluorescence when cultured with DRGs from WT, but not DKO, mice. Application of exogenous CGRPα at a saturating concentration (100-1000 nM) activates CGRP-sniffers in both conditions. **(H)** Quantification of fluorescence change in CGRP-sniffer cells in response to vehicle, capsaicin and CGRPα stimulation in WT and DKO mice. n=18 wells from 3 mice (2M, 1F) for WT, and n=18 wells from 3 mice (2M, 1F) for DKO. For (H), means were compared using repeated measures 2-way ANOVA, followed by post-hoc Sidak's test. Error bars denote standard error of the mean.

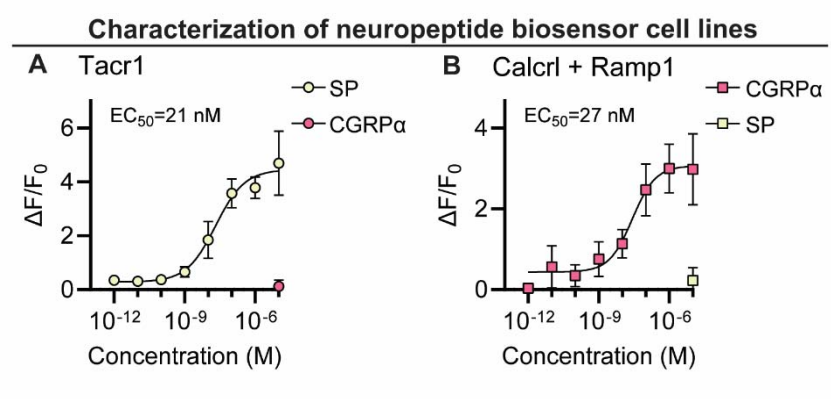

Figure 1 – figure supplement 1. Substance P-sniffer cells selectively respond to Substance P. (A) Dose-response curve showing Substance P activates Substance P-sniffer cells at low nanomolar concentrations (EC_{50}=11.8 nM), but cells are insensitive to CGRPα. **(B)** Dose-response curve showing CGRPα activates CGRP-sniffer cells at low nanomolar concentrations (EC_{50}=11.8 nM), but cells are insensitive to Substance P. 4-parameter variable slope dose-response curves were fit by non-linear regression. At least three replicates were performed for each concentration per condition, in two independent experiments.

2.2. Loss of Substance P and CGRPα does not affect acute pain or itch

To understand whether neuropeptide signaling is required for pain sensation, we performed a comprehensive battery of somatosensory behavior tests on DKO and wild-type control mice (WT). Notably, regardless of the type of mechanical or thermal stimulus, groups of animals showed no difference in their behavior (Figure 2). Specifically, responses to mechanical stimulation by von Frey hairs, pinpricks or an alligator clip were quantitatively indistinguishable (Figure 2A-C). In addition, withdrawal responses to radiant heat stimulation (Hargreaves', Figure 2D), and to two noxious Hot Plate temperatures were unaffected in DKO mice (Figure 2E). Responses to cold evoked by acetone and dry ice were also the same between groups (Figure 2F-G). Intraplantar injection of the Trpv1 agonist capsaicin evoked coping-like licking responses in both genotypes, however responses were variable and although decreased licking was observed in some DKO mice, differences did not reach statistical significance (Figure 2H). Therefore, to explore this potential difference using an independent measure, we quantified capsaicin-evoked Fos staining as a correlate of dorsal horn network activation. No differences in dorsal horn Fos expression were observed (Figure 2 – figure supplement 1A-B). Furthermore, intraplantar injection of a different algogen (the Trpa1 agonist allyl isothiocyanate, AITC) evoked similar licking behavior to capsaicin that was unaffected by peptide deletion (Figure 2I). Together these data suggest that loss of the two neuropeptides does not alter acute withdrawal or coping-like responses to multiple modalities of damaging stimuli applied to the paw.

We investigated whether dual peptide deletion might attenuate visceral pain. First, we dosed mice with acetic acid via intraperitoneal injection. This evoked comparable writhing behavior in both WT and DKO mice (Figure 2J). Next, because NKR1 antagonists are effective anti-emetics, we wondered whether the two peptides contribute to nausea-like behavior in mice (Warr et al., 2005). In many species, lithium chloride induces gastrointestinal malaise and when paired with a normally attractive tastant produces a marked conditioned taste aversion (Garcia et al., 1955). Notably, pairing saccharin with LiCl injection elicited a strong and indistinguishable conditioned taste aversion in both WT and DKO mice (Figure 2 – figure supplement 2A).

NKR1 antagonists have also been proposed to treat itch (Pojawa-Gołąb et al., 2019). Therefore, we examined whether peptide deletion abrogated itching. DKO mice scratched robustly following intradermal chloroquine injection, a response indistinguishable from WT animals (Figure

2K). Thus, our data demonstrate that Substance P and CGRPα contribute little to defensive behaviors evoked by diverse sensory stimuli.

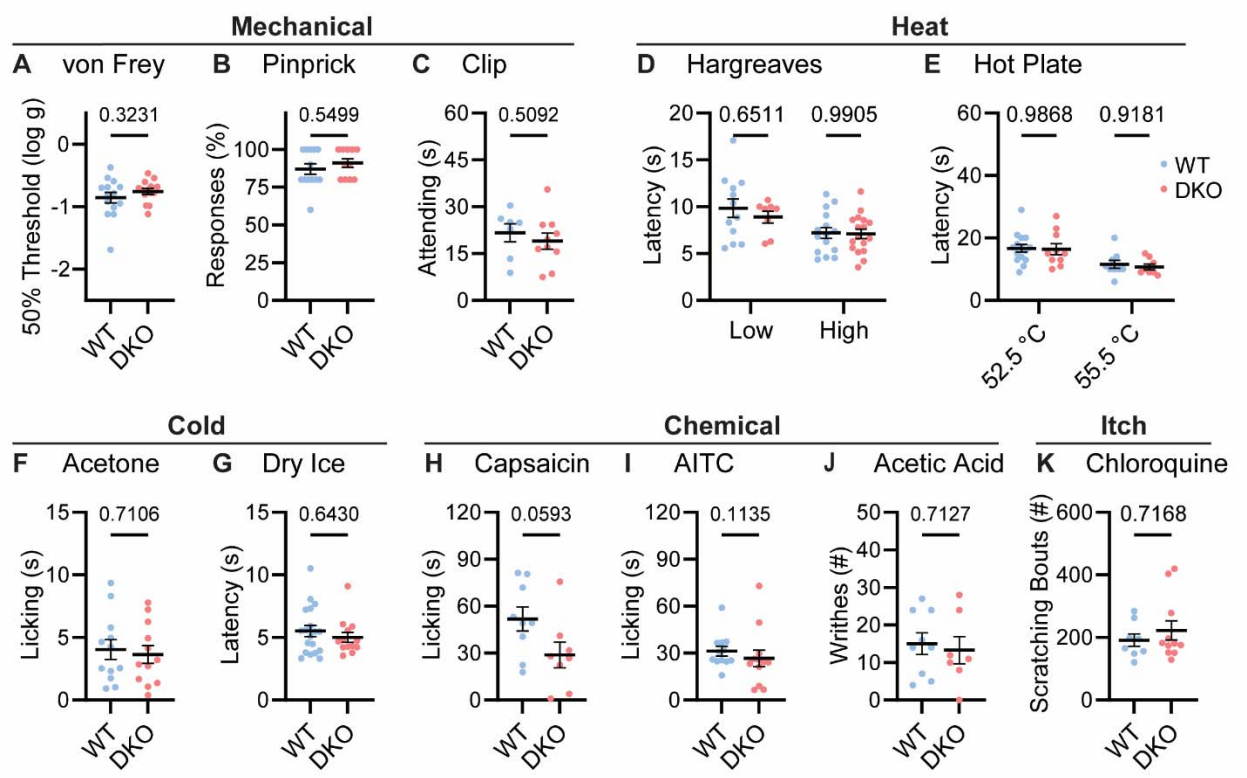

Figure 2. Tac1::Calca DKO mice respond to acute painful and itching stimuli. (**A**) 50% withdrawal threshold for von Frey punctate stimulation (log g). *n*=14 (7M, 7F) for WT & *n*=14 (7M, 7F) for DKO. (**B**) Percentage response to noxious pinprick stimulation. *n*=13 (5M, 8F) for WT & *n*=11 (4M, 7F) for DKO. **(C)** Time spent attending to alligator clip applied to paw for 60 s. *n*=7 (3M, 4F) for WT & *n*=10 (6M, 4F) for DKO. **(D)** Latency to withdraw to low and high radiant heat. For low setting, *n*=12 (6M, 6F) for WT & *n*=8 (4M, 4F) for DKO. For high setting, *n*=15 (8M, 7F) for WT & *n*=17 (9M, 8F) for DKO. **(E)** Latency to lick hindpaw following exposure to hot plate at two different temperatures. For 52.5 °C, *n*=15 (7M, 8F) for WT & *n*=10 (6M, 4F) for DKO. For 55.5 °C, *n*=9 (6M, 3F) for WT & *n*=8 (5M, 3F) for DKO. **(F)** Time spent licking in 60 s immediately following acetone application to paw. *n*=12 (5M, 7F) for WT & *n*=12 (5M, 7F) for DKO. (**D**) Latency to respond to dry ice. *n*=19 (8M, 11F) for WT & *n*=13 (5M, 8F) for DKO. (**H**) Time spent licking in 5 mins after capsaicin injection to paw. *n*=9 (4M, 5F) for WT & *n*=8 (4M, 4F) for DKO. (**I**) Time spent licking in 5 mins after 1% AITC injection to paw. *n*=12 (6M, 6F) for WT & *n*=12 (6M, 6F) for DKO. (**J**) Number of writhes in 15 mins starting 5 mins after intraperitoneal injection of 0.6% acetic acid. *n*=9 (5M, 4F) for WT & *n*=7 (5M, 2F) for DKO. (**K**) Scratching bouts in 15 minutes evoked by chloroquine injection into the nape of the neck. *n*=8 for WT & *n*=11 for DKO. For (A, C, F, H & J) means were compared using unpaired *t*-test, for (B, G, I and K) a Mann-Whitney U test was used, and for (D-E) a 2-Way ANOVA followed by post-hoc Sidak's test was used. Error bars denote standard error of the mean.

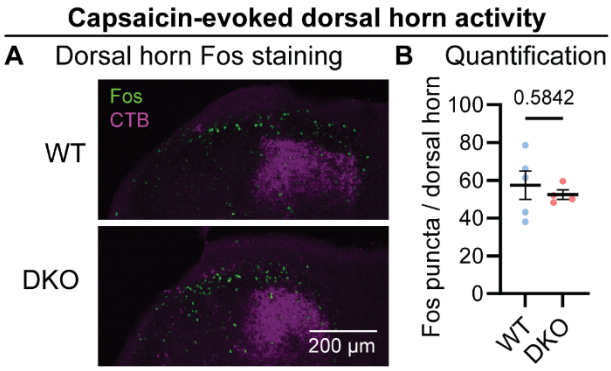

Figure 2 – figure supplement 1. Capsaicin evokes Fos activity in the dorsal horn of Tac1::Calca DKO mice. (A) Example confocal images showing dorsal horn of WT and DKO mice backlabelled with CTB (*magenta*) from the paw. Similar numbers of Fos puncta (*green*) are visible in the ipsilateral superficial dorsal horn of the WT and DKO cases. **(B)** Quantification of the mean number of Fos puncta in the ipsilateral dorsal horn of WT and DKO mice. For each mouse, the number of Fos puncta was counted in the 5 sections with the strongest CTB labelling and then averaged so that *n* is the number of mice. *n*=5 (2M, 3F) for WT & *n*=4 (2M, 2F) for DKO. Means were compared for (B) using an unpaired t test. Error bars denote standard error of the mean.

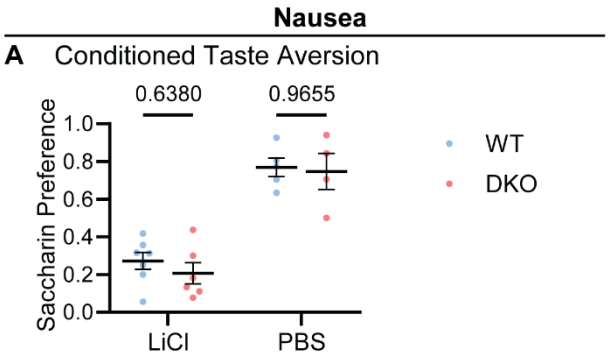

Figure 2 – figure supplement 2. Tac1::Calca DKO mice develop LiCl-induced conditioned taste aversion (A) Quantification of conditioned taste aversion (CTA) test in WT (blue) and DKO (red) mice. Saccharin preference index on test day is shown for animals given either lithium chloride or PBS following saccharin exposure on the conditioning day. Both WT and DKO treated with LiCl show a pronounced aversion to the usually-preferred saccharin. For LiCl, *n*=7 (4M, 3F) for WT & *n*=6 (4M, 2F) for DKO. For PBS, *n*=5 (3M, 2F) for WT & *n*=4 (2M, 2F) for DKO. Means were compared by 2-way ANOVA followed by post-hoc Sidak's test. Error bars denote standard error of the mean.

2.3. Inflammatory pain and neurogenic inflammation are preserved in Substance P and CGRPα-deficient mice

Chronic inflammatory pain results in long lasting changes in nociceptor function and the downstream pathways they engage. This plasticity is widely thought to involve neuropeptides (Zieglgänsberger, 2019). We therefore tested whether loss of Substance P and CGRPα impacted the development of heat hypersensitivity following treatment with Complete Freund's Adjuvant (CFA). Surprisingly, WT and DKO mice with intraplantar injection of CFA developed strong heat hypersensitivity (Figure 3A). Mechanical hypersensitivity was also unaffected by peptide loss (Figure 3B). CFA injection causes a long-term inflammatory immune response, therefore we also tested Prostaglandin E2 (PGE2), which can acutely sensitize nociceptors. PGE2 injection elicited short-lasting heat and mechanical hypersensitivity to a similar extent in both WT and DKO mice (Figure 3C-D). Together, these data indicate that Substance P and CGRPα are not required for the behavioral sensitization associated with both acute and chronic inflammation.

Release of vasoactive peptides including Substance P and CGRPα from nociceptor terminals has been proposed to drive neurogenic inflammation, encompassing oedema and extravasation (Chiu et al., 2012). Unexpectedly, we noticed that injection of the inflammatory mediators CFA and PGE2, as well as the algogens AITC and capsaicin, provoked swelling of the hindpaw of DKO mice to a similar extent as WT mice. To examine the development of neurogenic inflammation more rigorously, we measured paw volumes after capsaicin injection, and observed no appreciable differences in capsaicin-induced swelling between WT and DKO mice. (Figure 3E-F). In addition, using the Evans blue dye method, we found that plasma extravasation was intact in DKO mice (Figure 3G). Similar results were observed following AITC injection (Figure 3H-J). Therefore, Substance P and CGRPα are dispensable for some forms of neurogenic inflammation.

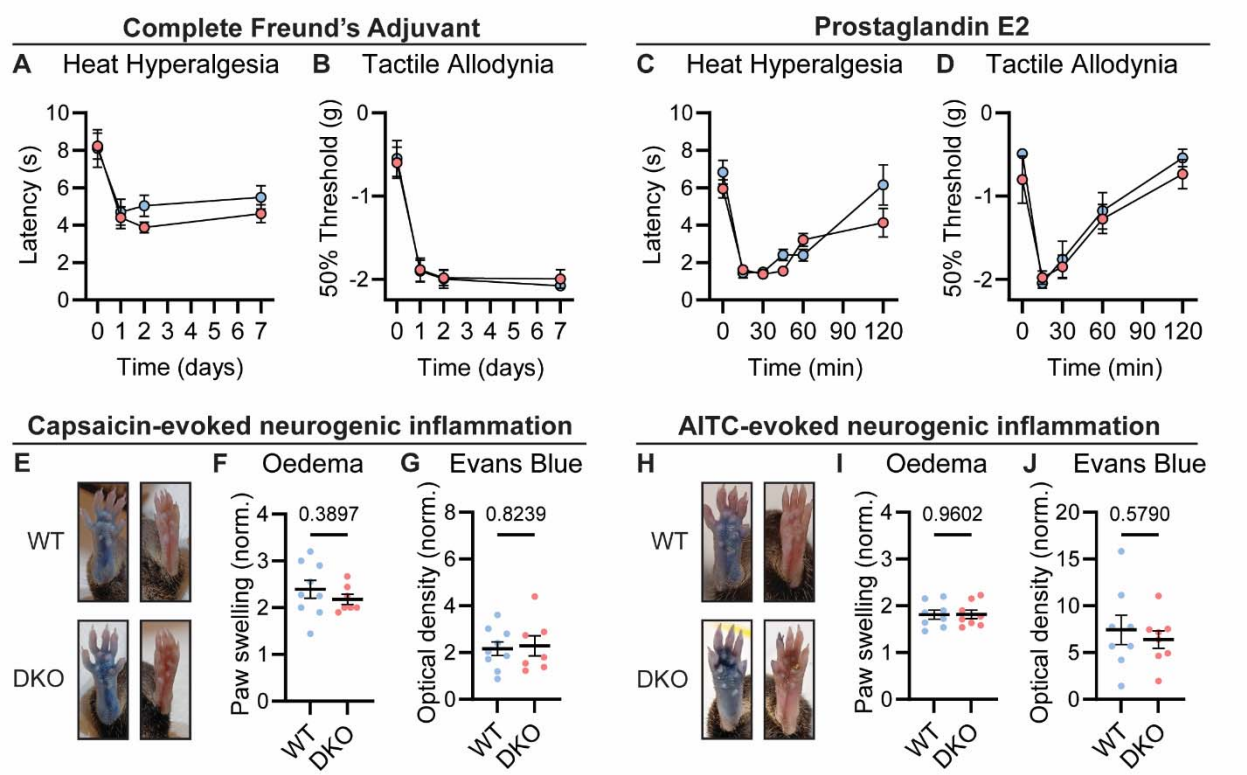

Figure 3. Tac1::Calca DKO mice display inflammatory pain and neurogenic inflammation. (A) Time course of the change in the Hargreaves' radiant heat withdrawal latencies of the hindpaw of WT and DKO mice following intraplantar injection of Complete Freund's Adjuvant (CFA). *n*=10 (5M, 5F) for WT & *n*=9 (4M, 5F) for DKO. **(B)** Time course of the change in von Frey 50% withdrawal thresholds (log g) on the hindpaw of WT and DKO mice after CFA. *n*=6 (3M, 3F) for WT & *n*=6 (3M, 3F) for DKO. **(C)** Time course of the change in the Hargreaves' radiant heat withdrawal latencies of the hindpaw of WT and DKO mice following intraplantar injection of Prostaglandin E2 (PGE2). *n*=10 (8M, 2F) for WT & *n*=10 (7M, 3F) for DKO. Post-hoc tests show only the 120 min time-point shows a significant difference (p=0.025). **(D)** Time course of the change in von Frey 50% withdrawal thresholds (log g) on the hindpaw of WT and DKO mice after PGE2. *n*=6 (3M, 3F) for WT & *n*=6 (3M, 3F) for DKO. **(E)** Images showing both WT and DKO mice show paw swelling and plasma extravasation following capsaicin injection (*left*) compared to uninjected paw (*right*). **(F)** Capsaicin-induced oedema, with injected paw swelling measured by volume and normalized to the uninjected paw, in WT and DKO mice. *n*=9 for WT (5M, 4F) & *n*=7 for DKO (4M, 3F). **(G)** Optical density of Evans blue dye extracted from the capsaicin-injected paw, normalized to uninjected paw, in WT and DKO mice. *n*=9 for WT (5M, 4F) & *n*=7 for DKO (4M, 3F). **(H)** Images showing both WT and DKO mice show paw swelling and plasma extravasation following AITC injection (*left*) compared to uninjected paw (*right*). **(I)** AITC-induced oedema, with injected paw swelling measured by volume and normalized to the uninjected paw, in WT and DKO mice. *n*=8 for WT (4M, 4F) & *n*=8 for DKO (4M, 4F). **(J)** Optical density of Evans blue dye extracted from AITC-injected paw, normalized to uninjected paw, in WT and DKO mice. *n*=8 for WT (4M, 4F) & *n*=8 for DKO (4M, 4F). For (A-D), means were compared using 2-way ANOVA followed by post-hoc Sidak's test, and for (F-G) and (I-J), an unpaired *t*-test was used. Error bars denote standard error of the mean.

2.4. Neuropathic pain is unaffected by Substance P and CGRPα deletion

Lastly, we investigated how dual peptide deletion affected the development of allodynia symptoms, where innocuous stimuli are perceived as painful, in two mouse models of neuropathic pain (Jensen and Finnerup, 2014). First, we performed a sciatic spared nerve injury on DKO animals and found that the static mechanical allodynia evoked by von Frey filaments developed to the same degree as in WT mice, persisting for three weeks (Figure 4A). Brush-evoked Fos activity in the superficial laminae of the dorsal horn of SNI-treated mice – a correlate of dynamic allodynia – was also comparable between genotypes (Figure 4B-C). Second, we treated mice with the chemotherapeutic drug oxaliplatin which evokes extreme cold allodynia that is known to depend, in part, on CGRPα-positive silent cold-sensing neurons (MacDonald et al., 2021). One day after intraplantar oxaliplatin treatment, both DKO and WT animals displayed pronounced pain-like behaviors when placed on a Cold Plate held at 10 °C (Figure 4D). Substance P and CGRPα are therefore not essential for mechanical or cold allodynia.

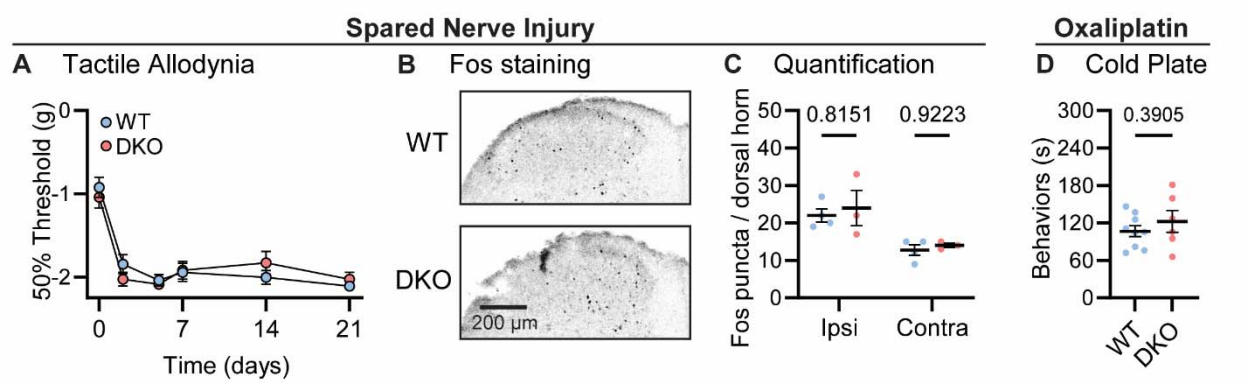

Figure 4. Tac1::Calca DKO mice develop neuropathic pain associated with nerve injury and the chemotherapeutic drug oxaliplatin. (A) Time course of the change in the von Frey 50% withdrawal threshold (log g) of the hindpaw of WT and DKO mice after sciatic spared nerve injury. *n*=8 (4M, 4F) for WT & *n*=8 (4M, 4F) for DKO. **(B)** Example confocal images showing Fos staining in the dorsal horn of WT and DKO mice following 30 minutes of brushing of the lateral part of the plantar surface of the hindpaw ipsilateral to the spared nerve injured. Fos puncta are visible in the ipsilateral dorsal horn of both WT and DKO cases. **(C)** Quantification of the mean number of Fos puncta in the ipsilateral and contralateral dorsal horn of WT and DKO mice. For each mouse, the number of Fos puncta was counted in 5 sections and then averaged so that *n* is the number of mice. *n*=4 for WT & *n*=3 for DKO. **(D)** Quantification of the time WT and DKO mice pre-treated with oxaliplatin (40 µg / 40 µl intraplantar) spent exhibiting pain-like behaviors in 5 minutes of exposure to a cold plate held at -10 °C. *n*=9 (5M, 4F) for WT & *n*=6 (3M, 3F) for DKO. Means were compared for (A) with a 2-Way ANOVA followed by post-hoc Sidak's test, and for (D) with an unpaired t test. Error bars denote standard error of the mean.

3. Discussion

The neuropeptides Substance P and CGRPα have been proposed to play diverse but largely overlapping roles in acute, inflammatory and neuropathic pain. However, when the levels of peptide signaling have been experimentally manipulated, effects have often been small and variable between studies, possibly due to redundancy (Hohmann et al., 2004). We therefore generated DKO mice lacking both Substance P and CGRPα signaling. Remarkably, both peptides were dispensable for pain across a wide range of assays.

It is difficult to reconcile our findings with the fact that Substance P and CGRPα are highly expressed throughout ascending pain pathways and are often found together in the same cells. (Pauli et al., 2022; Sharma et al., 2020; Zeisel et al., 2018). Studies of *Tac1* and *Calca* single KO mice reported significant impairments in acute pain, including heat sensitivity, visceral pain and the formalin test (Cao et al., 1998; Salmon et al., 2001, 1999; Zimmer et al., 1998). Notably, these deficits were modest, and in fact inconsistent between studies (Woolf et al., 1998; Zajdel et al., 2021). Nonetheless, ablating either peripheral or central neurons expressing Substance P and CGRPα produces profound analgesia (Barik et al., 2018; Cowie et al., 2018; Han et al., 2015; McCoy et al., 2013). Importantly, these neurons are all glutamatergic, and are thought to co-release neuropeptides to modulate synaptic transmission and neuronal firing (Pagani et al., 2019). Our work thus substantiates previous findings that established primary afferent-derived glutamate as the critical transmitter for most pain sensations (Lagerström et al., 2011, 2010; Liu et al., 2010; Rogoz et al., 2012; Scherrer et al., 2010), and suggests that the two peptides play at most a minor role.

An oft proposed caveat is that constitutive deletion of genes could be compensated for by upregulating the expression of functionally similar molecules, but with surprisingly little evidence (El-Brolosy and Stainier, 2017). Alternatively, neuropeptides may have opposing effects in different parts of the circuitry meaning global loss of the gene may produce a net effect of no change in a particular behavior. Indeed, classical studies show Substance P infusion into the spinal cord elicits pain, but paradoxically in the brain is analgesic (Hylden and Wilcox, 1981; Malick and Goldstein, 1978). Despite this, knockout of a gene remains the strongest test of whether the molecule it encodes is essential for a biological phenomenon (Caterina et al., 2000; Chesler et al., 2016; Mishra and Hoon, 2013), and our results clearly demonstrate that Substance P and CGRPα are not required for pain transmission.

The striking and highly-conserved pattern of expression of these two peptides in pain pathways, particularly in nociceptors, raises the question of why these neurons evolved to release them. Rather than directly acting as pain transmitters in the CNS, accumulating evidence indicates the secretion of these neuropeptides from nociceptor peripheral terminals modulates immune cells and the vasculature in diverse tissues (Chiu et al., 2013, 2012; Cohen et al., 2019; Lai et al., 2020; Perner et al., 2020; Pinho-Ribeiro et al., 2016; Yang et al., 2022). We focused on pain transmission, but it is clear our DKO mice will be useful reagents for exploring the crosstalk between nociceptors and other body systems. For example, the development of effective migraine therapeutics targeting CGRPα or its receptor confirm the important role this peptide plays in headache (De Matteis et al., 2020; Tso and Goadsby, 2017), and new efferent functions for both CGRPα and Substance P are regularly being uncovered (Brain, 1997; Caceres et al., 2009; Perner et al., 2020; Pinho-Ribeiro et al., 2016; Wilhelms et al., 2018; Yang et al., 2022).

Beyond Substance P and CGRPα, pain-responsive neurons express a rich repertoire of potential signaling molecules, including other neuropeptides. Emerging approaches to image and manipulate these molecules (Girven et al., 2022; Kim et al., 2024), as well as advances in quantitating pain behaviors (Bohic et al., 2023; MacDonald and Chesler, 2023), may ultimately reveal the fundamental roles of neuropeptides in generating our experience of pain.

4. Acknowledgements

We thank the National Center for Complementary and Integrative Health and the National Institute of Neurological Disorders and Stroke for providing funding. DIM was supported by a European Molecular Biology Organization Postdoctoral Fellowship, a Branco Weiss Fellowship – Society in Science, and an NIH Office of Autoimmune Disease Intramural Award. We are grateful to Nick Ryba and members of the Chesler lab for feedback and advice.

5. Declaration of interests

The authors declare no conflict of interests.

6. Materials and Methods

6.1. Animals

Animal care and experimental procedures were performed in accordance with a protocol approved by the National Institute for Neurological Diseases and Stroke (NINDS) Animal Care and Use Committee. DKO mice were generated by crossing B6.Cg-Calcatm1.1(cre/EGFP)Rpa/J (Jax #033168) with Tac1-tagRFP-2A-TVA (Carter et al., 2013; Wu et al., 2018). Control WT animals were C57/BL6j mice from The Jackson Laboratory (Jax #000664). Both male and female (>□6□weeks) mice were used for all experiments, and the number of mice of each sex used to generate each dataset is reported in the legend. The experimenter was blinded to genotype throughout. Genomic DNA was isolated from tail biopsy for genotyping by Transnetyx.

6.2. Immunohistochemistry

6.2.1. Substance P and CGRPα staining

Mice were anesthetized with isoflurane and perfused intracardially with heparin then 4% PFA. Tissue was post-fixed in 4% PFA overnight and then cryoprotected in 30% sucrose. Tissue was mounted in OCT and cut using a cryostat into 40-50 micron sections. The sections were incubated in a blocking buffer (5% donkey serum; 0.1% Triton X-100; PBS) for 3 hours at room temperature on a shaker. The sections were incubated in 1:500 goat anti-CGRP polyclonal primary antibody (Abcam, #ab36001) or 1:500 rabbit anti substance P polyclonal primary antibody (Abcam, #ab67006) at room temperature overnight. The sections were rinsed 2 times with PBS and then incubated for 2 hours in 1:200 Cy5-conjugated donkey anti-rabbit secondary antibody or 1:200 Cy5-conjugated donkey anti-goat secondary antibody (Thermo Fisher Scientific). The sections were rinsed 2 times with PBS and mounted in ProLong diamond antifade mounting media (Thermo Fisher Scientific) onto slides (Daigger Scientific). Z-stacks were acquired on an Olympus confocal microscope using a 20x objective and processed using ImageJ/FIJI software (National Institute of Health).

6.2.2. Fos staining for neuronal activity

Mice were injected with 10 microliters of 0.1% Alexa Fluor 647 conjugated cholera toxin subunit B into one hindpaw so that the most highly-innervated spinal cord sections could later be identified.

After 1 week, mice were habituated then the stimulation was performed. For capsaicin-evoked dorsal horn Fos, capsaicin (0.3%) was injected into the right hindpaw of mice in chambers on a plexiglass stand. For Fos elicited by dynamic allodynia stimulation, mice that received a spared nerve injury procedure 3 weeks prior were stimulated with a paint brush while housed on a wire mesh stand (3 x 10 min stimulation period, with 1 minute rest every 10 mins). Note that for SNI experiments, the CTB was injected into the contralateral paw, because severing two branches of the sciatic nerve would have prevented efficient CTB transit in the ipsilateral paw. The mice were perfused as above and spinal cords were harvested 75-120 mins after stimulation. The sections were incubated in a blocking buffer (5% goat serum; 0.1% Triton X-100; PBS) for 3 hours at room temperature on a shaker. The sections were incubated in 1:1000 rabbit anti Fos primary antibody (Cell Signaling Technology, Phospho-c-Fos (Ser32) (D82C12) XP® Rabbit mAb, #5348) at room temperature overnight. The sections were rinsed 2 times with PBS and incubated for 2 hours in 1:5000 Alexa Fluor 750 goat anti-rabbit secondary antibody (Life Technologies). The sections were rinsed 2 times with PBS and mounted in ProLong diamond antifade mounting media (Thermo Fisher Scientific) onto slides (Daigger Scientific). Z-stack images were acquired on an Olympus confocal microscope using a 20x objective. The five sections with the greatest Alexa Fluor 647 cholera toxin subunit B signal were imaged for each mouse. This ensured Fos activity was measured only in those sections strongly innervated by the hindpaw. The number of Fos positive nuclei in the dorsal horn were quantified in ImageJ/FIJI software (National Institute of Health) by a blinded observer using a semi-automated procedure. Briefly, brightness and contrast were uniformly adjusted for all images, then the 'Find Maxima' and 'Analyze particles' functions were used within a region of interest to identify Fos puncta. The list of puncta was then manually curated to generate a final estimate of the number of puncat within the region of interest. Fos puncta counts for the five sections were averaged for each mouse.

6.3. Neuropeptide Imaging

6.3.1. Generation and maintenance of Substance P and CGRP-sniffer cell lines

To generate the Substance P-sniffer cell line, we produced a mouse *Tacr1* DNA construct by gene synthesis (Epoch Life Science, GS66243-3). *Tacr1* was subcloned along with a synthesized human G-protein α-subunit gene $G_{\alpha 15}$ and *GCaMP6s* it into the lentiviral plasmid backbone pLV-CMV-PGK-

Hyg (Cellomics Technology, LVR-1046) to create the final lentiviral plasmid pLV-CMV-GCaMP6s-P2A-TACR1-T2A-hG15-PGK-Hyg. We used this plasmid to produce lentiviral particles (Vigene Biosciences) and infected them into human embryonic kidney cells at a multiplicity of infection of 20 following manufacturer's instructions. The Flp-In T-REx HEK293 cell line was used (Thermo Fisher Scientific, R78007). Stably expressing cells were isolated by treating with 200 μg/mL hygromycin B (Thermo Fisher Scientific, 10687010).

To generate the CGRP-sniffer cell lines, we produced mouse *Calcrl* and *Ramp1* DNA constructs by DNA synthesis (Epoch Life Science). *Calcrl* was subcloned along with a synthesized human G-protein α-subunit gene $G_{\alpha 15}$ and GCaMP6s into a dox-inducible backbone (GS66685-1). These were transfected into HEK293 cells using a PiggyBac transposase system and selected for using puromycin. These cells were then transfected with a plasmid pSBbi-Neo-cmv-TETo2-RAMP1 IRES-mTagBFP2-NLS and selected using geneticin. Doxycycline was then used to induce expression of both constructs, and cells were maintained in doxycycline.

The cell lines were maintained on polystyrene culture plates (Fisher Scientific, 07-200-80) in a 5% CO_2 humidified incubator at 37°C. The growth medium was changed every 2–3 days and consisted of DMEM/F12 (Fisher Scientific, 11330032) supplemented with 10% fetal bovine serum (Fisher Scientific, 26140079) and 200 μg/mL hygromycin B. Cells were passaged when they reached confluence, which was roughly twice per week, and were never propagated past 20 passages. For passaging, cells were rinsed in PBS (Fisher Scientific, 10010023) and then incubated in Accutase (Fisher Scientific, 00-4555-56) for ~5 min at 37°C to detach. Cells were collected in a 15 mL tube (Fisher Scientific, 12-565-268) and centrifuged at 300 rcf for 3 min to pellet. The supernatant was aspirated, and cells were resuspended in growth medium followed by plating in new polystyrene plates. Typical dilution ratios for passaging were between 1:3 and 1:20. For imaging, Substance P-sniffer cells were cultured onto 8-well glass slides, and imaged before they reached confluency.

6.3.2. Adult dorsal root ganglion culture and Substance P-sniffer co-culture

Dorsal root ganglia (DRG) were dissected from the entire length of the spinal column and then digested in a pre-equilibrated enzyme mix for 35-45 minutes (37 °C, 5% CO2). The enzyme mix consisted of Hanks' balanced salt solution containing collagenase (type XI; 5 mg/ml), dispase (10 mg/ml), HEPES (5 mM) and glucose (10 mM). DRGs were then gently centrifuged for 3 minutes at 300 revolutions per minute, the supernatant was discarded and replaced with warmed DMEM/F-12, supplemented with 10% fetal bovine serum (FBS). Next, DRGs were mechanically triturated with

three fire-polished glass Pasteur pipettes of gradually decreasing inner diameter. Dissociated cells were then centrifuged again at 300 revolutions per minute, the supernatant was discarded and cells were re-suspended in the required volume of DMEM supplemented with FBS and nerve growth factor (50 ng/ml). Finally, cells were plated onto 8-well glass slides coated with poly-L-lysine (1 mg/ml) and laminin (1 mg/ml), and incubated at 37 °C in 5% CO2. 24 hours later, Substance P-sniffer cells were resuspended in DMEM/F-12, supplemented with 10% fetal bovine serum (FBS) and nerve growth factor (50 ng/ml). 70,000 cells were dispensed into each imaging well containing DRG neurons, and incubated for at least a further 24 hours before imaging was performed.

6.3.3. In vitro imaging

Imaging was performed in Ringer's solution: 125 mM NaCl, 3 mM KCl, 5 mM $CaCl_2$, 1 mM $MgCl_2$, 10 mM glucose, and 10 mM HEPES (all from Sigma-Aldrich), adjusted to pH 7.3 with 1 M NaOH, and osmolality measured ~280 mmol/kg. SP-sniffer cells alone, or co-cultured with DRGs, were rinsed in Ringer's solution and imaged in Ringer's solution at room temperature on an Olympus IX73 inverted microscope using a pco.panda sCMOS back-illuminated camera at 2 frames per second. Tac1-RFP was excited at 560 nm LED and GCaMP6f at 488 nm. All imaging trials began with 15 s of baseline measurement and then the cells were treated with chemicals by micropipette. The chemicals used were capsaicin (10 μM) and Substance P amide (1 pM to 1μM). The peak $\Delta F/F_0$ was calculated to quantify the changes in fluorescence associated with chemical application, with F_0 defined as the mean fluorescence intensity of the entire field of view in the 5 s immediately preceding stimulation.

6.4. Behavioral Assays

6.4.1. Von Frey

Punctate mechanical sensitivity was measured using the up-down method of Chaplan to obtain a 50% withdrawal threshold (Chaplan et al., 1994). Mice were habituated on a mesh wire stand for 1 hour. A 0.16g Von Frey hair was applied to the plantar region of the paw for 2 s. A response was recorded when the mouse swiftly lifted its paw in response to the stimulus. A positive response resulted in application of a filament of lesser strength on the following trial, and no response in application of a stronger filament. To calculate the 50% withdrawal threshold, five responses surrounding the 50% threshold were obtained after the first change in response. The pattern of

responses was used to calculate the 50% threshold = $(10[\chi+\varkappa\delta])/10{,}000)$, where χ is the log of the final von Frey filament used, $\varkappa$ = tabular value for the pattern of responses and δ the mean difference between filaments used in log units. The log of the 50% threshold was used to calculate summary and test statistics.

6.4.2. Pinprick

Mice were habituated on a mesh wire stand for 1 hour. A 27-gauge needle was blunted and used to apply pressure to the hind paw. A withdrawal response was quantified as the mouse lifting the paw swiftly away from the blunted needle. The pinprick stimulation was repeated for 5 or 10 trials with 5-minute breaks inbetween. The percentage of withdrawal responses was calculated for each mouse.

6.4.3. Clip

Mice were habituated in opaque chambers on a plexiglass stand for 1 hour. The mouse was restrained and an alligator clip was applied to the hindpaw just in front of the heel. The mouse was returned to the chamber. The mouse's behavioral response was recorded from below using a video camera. After 60 s, the clip was removed. The amount of time the mouse spent attending the clip and associated paw was quantified post-hoc by a blinded observer. Attending was defined as biting/handling the clip, and biting/licking the paw.

6.4.4. Hargreaves

Mice were habituated on a plexiglass stand for 1 hour with the Hargreaves machine turned on in a dark room. The radiant heat stimulus was aimed for the centre of the plantar region of the mouse's hind paw. The active intensity of the low stimulus was 40 intensity units, and of the high stimulus 55. The response latency was recorded for 5 trials with 10-minute breaks in between each trial.

6.4.5. Hot/Cold Plate

The plate was set to the desired temperature. A camera set up with a mirror was used for better visibility of the mouse on the hot plate. A clear cylindrical tube was placed around the hot plate to ensure the mouse cannot escape. Once the hot plate reached the set temperature, the mouse was placed on the hot plate and the top of the cylinder was covered. At the cut-off time, the mouse was taken off the hot plate and placed back in the cage. The latency to lick was scored post-hoc using the recorded videos by a blinded observer.

6.4.6. Dry Ice

Mice were habituated on a plexiglass floor stand for 1 hour. A 2 ml plastic syringe was cut in half to allow for crushed dry ice to be compacted into the tube. The dry ice was pushed up against the glass where the mouse's hind paw was resting. Withdrawal latency was recorded with a stopwatch. 10 minutes were given in between each trial. The procedure was repeated 5 times and an average of the withdrawal latencies was calculated.

6.4.7. Acetone

Mice were habituated on a plexiglass floor stand for 1 hour. Mice were videotaped as acetone was applied to the plantar region of their hind paw. Acetone was applied using a custom-made applicator, consisting of a 1ml syringe and plastic well where acetone was pushed out to generate a droplet for applying to the paw. Behavior was scored post-hoc by a blinded observer and the total amount of time spent licking the paw in a 60 second time interval was recorded. The experiment was repeated for a second trial and average scores were used.

6.4.8. Chemical Algogens

Mice were habituated on a plexiglass stand for 1 hour. 0.3% capsaicin in 80% saline / 10% Tween-80 / 10% ethanol or 1% AITC in saline was injected into the plantar surface of the hind paw. The injected volume for both was 20 µl. Mice were video-taped for 5 minutes. A blinded observer scored the amount of time in seconds the mouse spent licking the injected paw in a 5-minute time period.

6.4.9. Acetic Acid

Mice were habituated on a plexiglass stand for 1 hour. 0.6% of acetic acid was injected intraperitoneally at a dose of 10 µl per gram weight of the animal. Mice were videotaped for 20 minutes. The number of writhes was quantified post-hoc by a blinded observer during a 15-minute interval between 5 and 20 minutes after injection.

6.4.10. Conditioned Taste Aversion

Mice were single-housed and habituated for 3 days to drink from two glass bottles with stainless-steel ball-bearing spouts. Mice then received 3 days of training, where they were water-deprived for 22 hours followed by 30 mins exposure to a single water-containing bottle, then 90 mins exposure to both bottles. On the conditioning day, after 22 hours of water deprivation, mice were exposed to a single bottle containing saccharin water (15 mM) for 45 mins. Mice were then injected with lithium chloride (200 mg/kg) or PBS, and then given ordinary water for 75 mins. The animals were then water deprived for a further 22 hours. On the test day, mice were simultaneously exposed to a bottle

containing water and a bottle containing saccharin for 45 mins. The volume of each solution consumed was measured by weighing the bottles before and after. To calculate the saccharin preference index of each animal, the volume of saccharin consumed was divided by the total of fluid consumed, with a value less than 0.5 indicating the development of an aversion to saccharin.

6.4.11. Chloroquine-induced itch

Hair from the nape of the mouse's neck was removed 2-3 days prior to behavioral experiments using VEET hair removal cream and the area thoroughly washed and moisturizing cream applied. Mice were habituated to transparent acrylic chambers (10cm x 10cm x 13cm) 30 minutes prior to injection. Post habituation, a blinded investigator injected 20 µl of 25 µM Chloroquine diphosphate salt (Sigma-Aldrich: C6628) solution in 0.9% saline intradermally into the nape of the neck using a 31G insulin syringe. Videos were quantified by a separate blinded investigator with a scratching bout counted each time the mouse attended to the injected area with the hind paw after the paw was removed from the floor or mouth.

6.4.12. Inflammatory Pain Models

CFA and PGE2 was purchased from Sigma. 20 µl of CFA was injected into the heel of the hind paw. PGE2 (20 µl, 500 nM) was injected into the plantar surface of the hindpaw, and behavior was assessed over the same time-frame that produces *in vivo* sensitization of nociceptor responses (up to 120 minutes). Inflammation-induced hypersensitivity was measured using the Hargreaves and the von Frey, as described above.

6.4.13. Spared Nerve Injury

The mouse was anesthetized with isofluorane. The mouse was placed under the nose cone, belly down, and the left hind limb area was shaved. The area was wiped clean with an ethanol wipe and coated with betadine. Once the mouse was unresponsive, a 1-inch horizontal cut was made in the skin right along the femur. Once the natural separation of muscles was located, a small scissor tool was used to puncture the fascia and separate out the muscles. Once the sciatic nerve was located, curved forceps were used to separate out the nerve from the muscle. The nerve was traced towards the knee until the branch of three nerves (perineal, tibial and sural) was found. The sural nerve was spared and the perineal and tibial nerves were cut. The mouse was sutured up and placed back in the homecage for recovery without postoperative analgesics. Mechanical allodynia was assessed using the von Frey assay from 2 to 21 days post surgery.

6.4.14. Oxaliplatin

Chemotherapy-induced neuropathy was induced in mice by intraplantar injection of oxaliplatin into the left hind paw (Deuis et al., 2013; MacDonald et al., 2021). Oxaliplatin was made up to a dose of 80 µg in 40 µl of 5% glucose solution, due to its instability in chloride-containing saline solution. The number of nocifensive behaviors in 5 mins was assessed on the Cold Plate held at 10 °C 24 hours later.

6.5. Neurogenic Inflammation

6.5.1. Evans Blue assay

Mice were anesthetized using isoflurane. 200 µl of Evans Blue dye was injected into the mouse's tail vein. 15 mins later, one hindpaw was injected with an algogen. After a further 30 mins, the volume of each paw was measured by displacement using a plethysmometer (Ugo Basile). Both paws were then cut at the ankle and placed in tubes in the oven at 55 °C for 24 hours to dry. 1 ml of formamide was then added to each paw and incubated for 4-6 days at 55 °C to extract the dye from the paw tissue. 50 µl samples of dye-infused formamide from each paw were then dispensed to a 96 well plate in duplicate, along with a range of Evans blue dilutions in formamide to generate a standard curve. The optical density of each sample was then measured using a plate-reader, and the concentration of Evans Blue per paw sample interpolated from the standard curve to generate an index of extravasation in that paw.

6.6. Statistical Analysis

A Shapiro-Wilk test was used to test the normality of the data. Data were then compared using two-way ANOVA with post-hoc Sidak's test, Student's unpaired t test or Mann-Whitney U Test. The α value was 0.05. For all experiments n is the number of animals, except Substance P and CGRP imaging where n is the number of wells. Error bars denote standard error of the mean throughout. No power analyses were used to determine sample sizes, but our sample sizes are similar to those from previous studies(Caterina et al., 2000; Lagerström et al., 2010; Liu et al., 2010; Nassar et al., 2004). Graphs were generated and statistical analysis was performed using GraphPad 8.0 software (Prism). All statistical tests and results are reported in Supplementary Table 1.

Supplementary Table 1. Summary of statistical tests.

Figure	Name	Variable (units)	N	Passed Shapiro-Wilk Test for Normality?	Test	Comparison	Statistic	P	Post hoc analysis	Comparison	P (adjusted)
1E	Substance P Release	NKR1 Activation (deltaF/F0)	WT: 12; DKO: 12		2-WAY RM ANOVA	Interaction	F (2, 44) = 3.718	0.0322	Sidak's multiple comparisons test	Vehicle - WT vs DKO	0.86
						Drug	F (1.569, 34.51) = 78.37	<0.0001		Capsaicin - WT vs DKO	0.013
						Genotype	F (1, 22) = 5.226	0.0322		SP - WT vs DKO	0.893
1H	CGRP Release	CLR Activation (deltaF/F0)	WT: 18; DKO: 18		2-WAY RM ANOVA	Interaction	F (2, 68) = 5.317	0.0072	Sidak's multiple comparisons test	Vehicle - WT vs DKO	0.499
						Drug	F (1.106, 37.61) = 22.49	0.0001		Capsaicin - WT vs DKO	2E-04
						Genotype	F (1, 34) = 0.006702	0.9352		CGRP - WT vs DKO	0.421
2A	von Frey	50% Threshold (log g)	WT: 14; DKO: 14	Yes (WT: W=0.9238, P=0.2495; DKO: W=0.9521, P=0.5943)	Unpaired t-test	WT vs DKO	t=1.007	0.3231			
2B	Pinprick	Response (%)	WT: 13; DKO: 11	No (WT: W=0.813, P=0.0098; DKO: W=0.7538, P=0.0023)	Mann Whitney U Test	WT vs DKO	U=59.5	0.5499			
2C	Clip	Attending (s)	WT: 7; DKO: 10	Yes (WT: W=0.8768, P=0.2127; DKO: W=0.9484, P=0.6502)	Unpaired t-test	WT vs DKO	t=0.6762	0.5092			
2D	Hargreaves	Latency (s)	Low - WT: 12; DKO: 8; High - WT: 15; DKO: 17		2-WAY ANOVA	Interaction	F (1, 48) = 0.3387	0.5633	Sidak's multiple comparisons test	Low - WT vs DKO	0.651
						Intensity	F (1, 48) = 9.597	0.0033		High - WT vs DKO	0.991
						Genotype	F (1, 48) = 0.5373	0.4671			
2E	Hot Plate	Latency (s)	52.5 - WT: 15; DKO: 10; 55.5 - WT: 9; DKO: 8		2-WAY ANOVA	Interaction	F (1, 38) = 0.03579	0.851	Sidak's multiple comparisons test	52.5 - WT vs DKO	0.987
						Intensity	F (1, 38) = 14.27	0.0005		55.5 - WT vs DKO	0.918
						Genotype	F (1, 38) = 0.1417	0.7087			
2F	Acetone	Licking (s)	WT: 12; DKO: 12	Yes (WT: W=0.9097, P=0.2113; DKO: W=9371, P=0.4616)		WT vs DKO	t=0.3759	0.7106			
2G	Dry Ice	Latency (s)	WT: 19; DKO: 13	No (WT: W=0.9051, P=0.0602; DKO: W=0.7896, P=0.0051)	Mann Whitney U Test	WT vs DKO	U=111	0.643			
2H	Capsaicin	Licking (s)	WT: 9; DKO: 8	Yes (WT: W=0.926, P=0.4439; DKO: W=0.9062, P=0.3278)		WT vs DKO	t=2.041	0.0593			

Figure	Name	Variable (units)	N	Passed Shapiro-Wilk Test for Normality?	Test	Comparison	Statistic	P	Post hoc analysis	Comparison	P (adjusted)
2I	AITC	Licking (s)	WT: 12; DKO: 12	No (WT: W=0.8549, P=0.0422; DKO: W=0.8314, P=0.0218)		WT vs DKO	U=44	0.1135			
2J	Acetic Acid	Writhes (#)	WT: 9; DKO: 7	Yes (WT: W=0.9108, P=0.3214; DKO: W=9211, P=0.4778)		WT vs DKO	t=0.3757	0.7127			
2K	Chloroquine	Scratching Bouts (#)	WT: 8; DKO: 11	No (WT: W=0.9211, P=0.4392; DKO: W=0.7614, P=0.0029)			U=39	0.7168			
2-S1	Capsaicin Fos	Fos puncta / dorsal horn (#)	WT: 5; DKO: 4	Yes (WT: W=0.9444, P=0.6974; DKO: W=0.8844, P=0.3597)			t=0.5736	0.5842			
2-S2	Conditioned Taste Aversion	Latency (s)	LiCl- WT: 7; DKO: 6; PBS - WT: 5; DKO: 4		2-WAY ANOVA	Interaction	F (1, 18) = 0.1361	0.7165	Sidak's multiple comparisons test	LiCl	0.638
						Intensity	F (1, 18) = 75.79	<0.0001		PBS	0.966
						Genotype	F (1, 18) = 0.5413	0.4714			
3A	CFA -- Hargreaves	Latency (s)	WT: 9; DKO: 10		2-WAY RM ANOVA	Interaction	F (3, 51) = 0.4715	0.7035	Sidak's multiple comparisons test	0d - WT v DKO	>0.9999
						Time	F (2.117, 35.99) = 17.63	<0.0001		1d - WT v DKO	0.996
						Genotype	F (1, 17) = 0.8594	0.3669		2d - WT v DKO	0.334
										7d - WT v DKO	0.734
3B	CFA - von Frey	Threshold (log g)	WT: 6; DKO: 6		2-WAY RM ANOVA	Interaction	F (3, 30) = 0.07568	0.9726	Sidak's multiple comparisons test	0d - WT v DKO	0.998
						Time	F (3, 30) = 50.74	<0.0001		1d - WT v DKO	>0.9999
						Genotype	F (1, 10) = 0.02549	0.8763		2d - WT v DKO	>0.9999
										7d - WT v DKO	0.989
3C	PGE2 - Hargreaves	Latency (s)	WT: 10; DKO: 10		2-WAY RM ANOVA	Interaction	F (5, 90) = 2.053	0.0787	Sidak's multiple comparisons test	0m - WT vs DKO	0.738
						Time	F (5, 90) = 35.65	0.0001		15m - WT vs DKO	>0.9999
						Genotype	F (1, 18) = 3.020	0.0993		30m - WT vs DKO	>0.9999
										45m - WT vs DKO	0.765
										60m - WT vs DKO	0.804
										120m - WT vs DKO	0.025

Figure	Name	Variable (units)	N	Passed Shapiro-Wilk Test for Normality?	Test	Comparison	Statistic	P	Post hoc analysis	Comparison	P (adjusted)
3D	PGE2 - von Frey	Threshold (log g)	WT: 6; DKO: 6		2-WAY RM ANOVA	Interaction	F (4, 40) = 0.3472	0.8444	Sidak's multiple comparisons test	0m - WT vs DKO	0.856
						Time	F (2.803, 28.03) = 28.64	<0.0001		15m - WT vs DKO	0.977
						Genotype	F (1, 10) = 1.475	0.2525		30m - WT vs DKO	0.999
										45m - WT vs DKO	0.999
										60m - WT vs DKO	0.9
										120m - WT vs DKO	0.025
3F	Capsaicin - Oedema	Swelling (norm.)	WT: 9; DKO: 7	Yes (WT: W=0.9684, P=0.8811; DKO: W=0.8609, P=0.1541)	Unpaired t-test	WT vs DKO	t=0.8876	0.3897			
3G	Capsaicin - Extravasation	Optical Density (norm.)	WT: 9; DKO: 7	Yes (WT: W=0.9829, P=0.9776; DKO: W=0.8732, P=0.1981)	Unpaired t-test	WT vs DKO	t=0.2268	0.8239			
3I	AITC - Oedema	Swelling (norm.)	WT: 8; DKO: 8	Yes (WT: W=0.9428, P=0.639; DKO: W=0.8994, P=0.2853)	Unpaired t-test	WT vs DKO	t=0.05078	0.9602			
3J	AITC - Extravasation	Optical Density (norm.)	WT: 8; DKO: 8	Yes (WT: W=0.9459, P=0.6697; DKO: W=0.9597, P=0.8076)	Unpaired t-test	WT vs DKO	t=0.5681	0.579			
4A	SNI - Tactile Allodynia	Threshold (log g)	WT: 8; DKO: 8		2-WAY RM ANOVA	Interaction	F (5, 70) = 1.161	P=0.3370	Sidak's multiple comparisons test	0d - WT v DKO	0.952
						Time	F (5, 70) = 46.15	P<0.0001		2d - WT v DKO	0.731
						Genotype	F (1, 14) = 0.01651	P=0.8996		5d - WT v DKO	1
										7d - WT v DKO	>0.9999
										14d - WT v DKO	0.753
										21d - WT v DKO	0.991
4C	SNI - Fos staining	Fos puncta / dorsal horn (#)	WT: 4; DKO: 3		2-WAY ANOVA	Interaction	F (1, 5) = 0.02824	0.8731	Sidak's multiple comparisons test	Ipsi - WT vs DKO	0.815
						Side	F (1, 5) = 18.60	0.0076		Contra - WT vs DKO	0.922
						Genotype	F (1, 5) = 0.3993	0.5552			
4D	Oxaliplatin - Cold Plate	Behaviors (s)	WT: 9; DKO: 3	Yes (WT: W=0.9402, P=0.5843; DKO: W=0.9756, P=0.9274)	Unpaired t-test	WT vs DKO	t=0.8884	0.3905			

7. References

Amara SG, Jonas V, Rosenfeld MG, Ong ES, Evans RM. 1982. Alternative RNA processing in calcitonin gene expression generates mRNAs encoding different polypeptide products. *Nature* **298**:240–244. doi:10.1038/298240A0

Barik A, Thompson JH, Seltzer M, Ghitani N, Chesler AT. 2018. A Brainstem-Spinal Circuit Controlling Nocifensive Behavior. *Neuron* **100**:1491-1503.e3. doi:10.1016/j.neuron.2018.10.037

Bohic M, Pattison LA, Jhumka ZA, Rossi H, Thackray JK, Ricci M, Mossazghi N, Foster W, Ogundare S, Twomey CR, Hilton H, Arnold J, Tischfield MA, Yttri EA, St. John Smith E, Abdus-Saboor I, Abraira VE. 2023. Mapping the neuroethological signatures of pain, analgesia, and recovery in mice. *Neuron*. doi:10.1016/J.NEURON.2023.06.008

Brain SD. 1997. Sensory neuropeptides: their role in inflammation and wound healing. *Immunopharmacology* **37**:133–152. doi:10.1016/S0162-3109(97)00055-6

Caceres AI, Brackmann M, Elia MD, Bessac BF, Del Camino D, D'Amours M, Witek JAS, Fanger CM, Chong JA, Hayward NJ, Homer RJ, Cohn L, Huang X, Moran MM, Jordt SE. 2009. A sensory neuronal ion channel essential for airway inflammation and hyperreactivity in asthma. *Proc Natl Acad Sci U S A* **106**. doi:10.1073/pnas.0900591106

Cao YQ, Mantyh PW, Carlson EJ, Gillespie AM, Epstein CJ, Basbaum AI. 1998. Primary afferent tachykinins are required to experience moderate to intense pain. *Nature 1998 392:6674* **392**:390–394. doi:10.1038/32897

Carter ME, Soden ME, Zweifel LS, Palmiter RD. 2013. Genetic identification of a neural circuit that suppresses appetite. *Nature 2013 503:7474* **503**:111–114. doi:10.1038/nature12596

Caterina MJ, Leffler A, Malmberg AB, Martin WJ, Trafton J, Petersen-Zeitz KR, Koltzenburg M, Basbaum AI, Julius D. 2000. Impaired nociception and pain sensation in mice lacking the capsaicin receptor. *Science* **288**:306–13.

Chaplan SR, Bach FW, Pogrel JW, Chung JM, Yaksh TL. 1994. Quantitative assessment of tactile allodynia in the rat paw. *J Neurosci Methods* **53**:55–63.

Chen JY, Campos CA, Jarvie BC, Palmiter RD. 2018. Parabrachial CGRP Neurons Establish and Sustain Aversive Taste Memories. *Neuron* **100**:891-899.e5. doi:10.1016/J.NEURON.2018.09.032

Chesler A, Szczot M, Bharucha-Goebel D, Čeko M, Donkervoort S, Laubacher C, Hayes L, Alter K, Zampieri C, Stanley C, Innes A, Mah J, Grosmann C, Bradley N, Nguyen D, Foley A, Le Pichon C, Bönnemann C. 2016. The Role of PIEZO2 in Human Mechanosensation. *N Engl J Med* **375**. doi:10.1056/NEJMOA1602812

Chiu IM, Heesters BA, Ghasemlou N, Von Hehn CA, Zhao F, Tran J, Wainger B, Strominger A, Muralidharan S, Horswill AR, Wardenburg JB, Hwang SW, Carroll MC, Woolf CJ. 2013. Bacteria activate sensory neurons that modulate pain and inflammation. *Nature* **501**:52–57. doi:10.1038/nature12479

Chiu IM, Von Hehn CA, Woolf CJ. 2012. Neurogenic inflammation and the peripheral nervous system in host defense and immunopathology. *Nat Neurosci*. doi:10.1038/nn.3144

Cohen JA, Edwards TN, Liu AW, Hirai T, Jones MR, Wu J, Li Y, Zhang S, Ho J, Davis BM, Albers KM, Kaplan DH. 2019. Cutaneous TRPV1+ Neurons Trigger Protective Innate Type 17 Anticipatory Immunity. *Cell* **178**:919-932.e14. doi:10.1016/j.cell.2019.06.022

Cowie AM, Moehring F, O'Hara C, Stucky CL. 2018. Optogenetic Inhibition of CGRPα Sensory Neurons Reveals Their Distinct Roles in Neuropathic and Incisional Pain. *J Neurosci* **38**:5807–5825. doi:10.1523/JNEUROSCI.3565-17.2018

De Felipe C, Herrero JF, O'Brien JA, Palmer JA, Doyle CA, Smith AJH, Laird JMA, Belmonte C, Cervero F, Hunt SP. 1998. Altered nociception, analgesia and aggression in mice lacking the receptor for substance P. *Nature* **392**. doi:10.1038/32904

De Matteis E, Guglielmetti M, Ornello R, Spuntarelli V, Martelletti P, Sacco S. 2020. Targeting CGRP for migraine treatment: mechanisms, antibodies, small molecules, perspectives. *https://doi.org/101080/1473717520201772758* **20**:627–641. doi:10.1080/14737175.2020.1772758

Deuis JR, Zimmermann K, Romanovsky AA, Possani LD, Cabot PJ, Lewis RJ, Vetter I. 2013. An animal model of oxaliplatin-induced cold allodynia reveals a crucial role for Nav1.6 in peripheral pain pathways. *Pain* **154**:1749–57. doi:10.1016/j.pain.2013.05.032

Drucker DJ. 2022. GLP-1 physiology informs the pharmacotherapy of obesity. *Mol Metab*. doi:10.1016/j.molmet.2021.101351

El-Brolosy MA, Stainier DYR. 2017. Genetic compensation: A phenomenon in search of mechanisms. *PLoS Genet*. doi:10.1371/journal.pgen.1006780

Garcia J, Kimeldorf DJ, Koelling RA. 1955. Conditioned Aversion to Saccharin Resulting from Exposure to Gamma Radiation. *Science (1979)* **122**. doi:10.1126/science.122.3160.157

Girven KS, Mangieri L, Bruchas MR. 2022. Emerging approaches for decoding neuropeptide transmission. *Trends Neurosci* **45**:899–912. doi:10.1016/j.tins.2022.09.005

Guo TZ, Wei T, Shi X, Li WW, Hou S, Wang L, Tsujikawa K, Rice KC, Cheng K, Clark DJ, Kingery WS. 2012. Neuropeptide deficient mice have attenuated nociceptive, vascular, and inflammatory changes in a tibia fracture model of complex regional pain syndrome. *Mol Pain* **8**. doi:10.1186/1744-8069-8-85

Han S, Soleiman M, Soden M, Zweifel L, Palmiter RD. 2015. Elucidating an Affective Pain Circuit that Creates a Threat Memory. *Cell* **162**:363–374. doi:10.1016/j.cell.2015.05.057

Hill R. 2000. NK1 (substance P) receptor antagonists - Why are they not analgesic in humans? *Trends Pharmacol Sci* **21**:244–246. doi:10.1016/S0165-6147(00)01502-9

Hohmann JG, Teklemichael DN, Weinshenker D, Wynick D, Clifton DK, Steiner RA. 2004. Obesity and Endocrine Dysfunction in Mice with Deletions of both Neuropeptide Y and Galanin. *Mol Cell Biol* **24**. doi:10.1128/mcb.24.7.2978-2985.2004

Huang T, Lin SH, Malewicz NM, Zhang Yan, Zhang Ying, Goulding M, LaMotte RH, Ma Q. 2019. Identifying the pathways required for coping behaviours associated with sustained pain. *Nature* **565**:86–90. doi:10.1038/s41586-018-0793-8

Hylden JLK, Wilcox GL. 1981. Intrathecal substance P elicits a caudally-directed biting and scratching behavior in mice. *Brain Res* **217**. doi:10.1016/0006-8993(81)90203-1

Jensen TS, Finnerup NB. 2014. Allodynia and hyperalgesia in neuropathic pain: clinical manifestations and mechanisms. *Lancet Neurol* **13**:924–935. doi:10.1016/S1474-4422(14)70102-4

Jin Y, Smith C, Monteith D, Brown R, Camporeale A, McNearney TA, Deeg MA, Raddad E, Xiao N, de la Peña A, Kivitz AJ, Schnitzer TJ. 2018. CGRP blockade by galcanezumab was not associated with reductions in signs and symptoms of knee osteoarthritis in a randomized clinical trial. *Osteoarthritis Cartilage* **26**:1609–1618. doi:10.1016/J.JOCA.2018.08.019

Kang SJ, Liu S, Ye M, Kim D Il, Pao GM, Copits BA, Roberts BZ, Lee KF, Bruchas MR, Han S. 2022. A central alarm system that gates multi-sensory innate threat cues to the amygdala. *Cell Rep* **40**. doi:10.1016/j.celrep.2022.111222

Kim D Il, Park Sekun, Park Seahyung, Ye M, Chen JY, Kang SJ, Jhang J, Hunker AC, Zweifel LS, Caron KM, Vaughan JM, Saghatelian A, Palmiter RD, Han S. 2024. Presynaptic sensor and silencer of peptidergic transmission reveal neuropeptides as primary transmitters in pontine fear circuit. *Cell* **187**:5102-5117.e16. doi:10.1016/J.CELL.2024.06.035/ASSET/8E4A614E-33D7-4028-8D28-CE5571AA986C/MAIN.ASSETS/FIGS5_LRG.JPG

Lagerström MC, Rogoz K, Abrahamsen B, Lind AL, Ölund C, Smith C, Mendez JA, Wallén-Mackenzie Å, Wood JN, Kullander K. 2011. A sensory subpopulation depends on vesicular glutamate transporter

2 for mechanical pain, and together with substance P, inflammatory pain. *Proc Natl Acad Sci U S A* **108**:5789–5794. doi:10.1073/pnas.1013602108

Lagerström MC, Rogoz K, Abrahamsen B, Persson E, Reinius B, Nordenankar K, Ölund C, Smith C, Mendez JA, Chen ZF, Wood JN, Wallén-Mackenzie Å, Kullander K. 2010. VGLUT2-Dependent Sensory Neurons in the TRPV1 Population Regulate Pain and Itch. *Neuron* **68**. doi:10.1016/j.neuron.2010.09.016

Lai NY, Musser MA, Pinho-Ribeiro FA, Baral P, Jacobson A, Ma P, Potts DE, Chen Z, Paik D, Soualhi S, Yan Y, Misra A, Goldstein K, Lagomarsino VN, Nordstrom A, Sivanathan KN, Wallrapp A, Kuchroo VK, Nowarski R, Starnbach MN, Shi H, Surana NK, An D, Wu C, Huh JR, Rao M, Chiu IM. 2020. Gut-Innervating Nociceptor Neurons Regulate Peyer's Patch Microfold Cells and SFB Levels to Mediate Salmonella Host Defense. *Cell* **180**:33-49.e22. doi:10.1016/j.cell.2019.11.014

Latremoliere A, Woolf CJ. 2009. Central Sensitization: A Generator of Pain Hypersensitivity by Central Neural Plasticity. *Journal of Pain*. doi:10.1016/j.jpain.2009.06.012

Lein ES, Hawrylycz MJ, Ao N, Ayres M, Bensinger A, Bernard A, Boe AF, Boguski MS, Brockway KS, Byrnes EJ, Chen Lin, Chen Li, Chen TM, Chin MC, Chong J, Crook BE, Czaplinska A, Dang CN, Datta S, Dee NR, Desaki AL, Desta T, Diep E, Dolbeare TA, Donelan MJ, Dong HW, Dougherty JG, Duncan BJ, Ebbert AJ, Eichele G, Estin LK, Faber C, Facer BA, Fields R, Fischer SR, Fliss TP, Frensley C, Gates SN, Glattfelder KJ, Halverson KR, Hart MR, Hohmann JG, Howell MP, Jeung DP, Johnson RA, Karr PT, Kawal R, Kidney JM, Knapik RH, Kuan CL, Lake JH, Laramee AR, Larsen KD, Lau C, Lemon TA, Liang AJ, Liu Y, Luong LT, Michaels J, Morgan JJ, Morgan RJ, Mortrud MT, Mosqueda NF, Ng LL, Ng R, Orta GJ, Overly CC, Pak TH, Parry SE, Pathak SD, Pearson OC, Puchalski RB, Riley ZL, Rockett HR, Rowland SA, Royall JJ, Ruiz MJ, Sarno NR, Schaffnit K, Shapovalova N V., Sivisay T, Slaughterbeck CR, Smith SC, Smith KA, Smith BI, Sodt AJ, Stewart NN, Stumpf KR, Sunkin SM, Sutram M, Tam A, Teemer CD, Thaller C, Thompson CL, Varnam LR, Visel A, Whitlock RM, Wohnoutka PE, Wolkey CK, Wong VY,

Wood M, Yaylaoglu MB, Young RC, Youngstrom BL, Yuan XF, Zhang B, Zwingman TA, Jones AR. 2007. Genome-wide atlas of gene expression in the adult mouse brain. *Nature* **445**. doi:10.1038/nature05453

Liu Y, Abdel Samad O, Zhang L, Duan B, Tong Q, Lopes C, Ji RR, Lowell BB, Ma Q. 2010. VGLUT2-Dependent Glutamate Release from Nociceptors Is Required to Sense Pain and Suppress Itch. *Neuron* **68**:543–556. doi:10.1016/j.neuron.2010.09.008

Löken LS, Braz JM, Etlin A, Sadeghi M, Bernstein M, Jewell M, Steyert M, Kuhn J, Hamel K, Llewellyn-Smith IJ, Basbaum A. 2021. Contribution of dorsal horn cgrp-expressing interneurons to mechanical sensitivity. *Elife* **10**. doi:10.7554/eLife.59751

MacDonald DI, Chesler AT. 2023. Painspotting. *Neuron* **111**:2773–2774. doi:10.1016/j.neuron.2023.08.026

MacDonald DI, Luiz AP, Iseppon F, Millet Q, Emery EC, Wood JN. 2021. Silent cold-sensing neurons contribute to cold allodynia in neuropathic pain. *Brain*. doi:10.1093/brain/awab086

Malick JB, Goldstein JM. 1978. Analgesic activity of substance P following intracerebral administration in rats. *Life Sci* **23**. doi:10.1016/0024-3205(78)90518-0

McCoy ES, Taylor-Blake B, Street SE, Pribisko AL, Zheng J, Zylka MJ. 2013. Peptidergic CGRPα Primary Sensory Neurons Encode Heat and Itch and Tonically Suppress Sensitivity to Cold. *Neuron* **78**. doi:10.1016/j.neuron.2013.01.030

Mishra SK, Hoon MA. 2013. The cells and circuitry for itch responses in mice. *Science (1979)* **340**. doi:10.1126/science.1233765

Nahin RL, Feinberg T, Kapos FP, Terman GW. 2023. Estimated Rates of Incident and Persistent Chronic Pain Among US Adults, 2019-2020. *JAMA Netw Open* **6**:e2313563. doi:10.1001/JAMANETWORKOPEN.2023.13563

Nassar MA, Stirling LC, Forlani G, Baker MD, Matthews EA, Dickenson AH, Wood JN. 2004. Nociceptor-specific gene deletion reveals a major role for Nav1.7 (PN1) in acute and inflammatory pain. *Proc Natl Acad Sci U S A* **101**:12706–11. doi:10.1073/pnas.0404915101

Nguyen MQ, von Buchholtz LJ, Reker AN, Ryba NJP, Davidson S. 2021. Single-nucleus transcriptomic analysis of human dorsal root ganglion neurons. *Elife* **10**. doi:10.7554/ELIFE.71752

Ogunlaja OI, Goadsby PJ. 2022. Headache: Treatment update. *eNeurologicalSci*. doi:10.1016/j.ensci.2022.100420

Pagani M, Albisetti GW, Sivakumar N, Wildner H, Santello M, Johannssen HC, Ulrich H, Correspondence Z. 2019. How Gastrin-Releasing Peptide Opens the Spinal Gate for Itch. *Neuron* **103**:102–117. doi:10.1016/j.neuron.2019.04.022

Paige C, Plasencia-Fernandez I, Kume M, Papalampropoulou-Tsiridou M, Lorenzo LE, David ET, He L, Mejia GL, Driskill C, Ferrini F, Feldhaus AL, Garcia-Martinez LF, Akopian AN, De Koninck Y, Dussor G, Price TJ. 2022. A Female-Specific Role for Calcitonin Gene-Related Peptide (CGRP) in Rodent Pain Models. *Journal of Neuroscience* **42**. doi:10.1523/JNEUROSCI.1137-21.2022

Palmiter RD. 2018. The Parabrachial Nucleus: CGRP Neurons Function as a General Alarm. *Trends Neurosci*. doi:10.1016/j.tins.2018.03.007

Park TJ, Comer C, Carol A, Lu Y, Hong HS, Rice FL. 2003. Somatosensory organization and behavior in naked mole-rats: II. Peripheral structures, innervation, and selective lack of neuropeptides associated with thermoregulation and pain. *Journal of Comparative Neurology* **465**. doi:10.1002/cne.10824

Park TJ, Lu Y, Jüttner R, Smith ESJ, Hu J, Brand A, Wetzel C, Milenkovic N, Erdmann B, Heppenstall PA, Laurito CE, Wilson SP, Lewin GR. 2008. Selective inflammatory pain insensitivity in the African naked mole-rat (Heterocephalus glaber). *PLoS Biol* **6**. doi:10.1371/journal.pbio.0060013

Pauli JL, Chen JY, Basiri ML, Park S, Carter ME, Sanz E, Stanley Mcknight G, Stuber GD, Palmiter RD. 2022. Molecular and anatomical characterization of parabrachial neurons and their axonal projections. *Elife* **11**. doi:10.7554/ELIFE.81868

Perner C, Flayer CH, Zhu X, Aderhold PA, Dewan ZNA, Voisin T, Camire RB, Chow OA, Chiu IM, Sokol CL. 2020. Substance P Release by Sensory Neurons Triggers Dendritic Cell Migration and Initiates the Type-2 Immune Response to Allergens. *Immunity* **53**:1063-1077.e7. doi:10.1016/j.immuni.2020.10.001

Pinho-Ribeiro FA, Verri WA, Chiu IM. 2016. Nociceptor Sensory Neuron–Immune Interactions in Pain and Inflammation Modulation of Pain Sensitivity by Immune Cells. *Trends Immunol* **xx**.

Pojawa-Gołąb M, Jaworecka K, Reich A. 2019. NK-1 Receptor Antagonists and Pruritus: Review of Current Literature. *Dermatol Ther (Heidelb)*. doi:10.1007/s13555-019-0305-2

Rogoz K, Lagerström MC, Dufour S, Kullander K. 2012. VGLUT2-dependent glutamatergic transmission in primary afferents is required for intact nociception in both acute and persistent pain modalities. *Pain* **153**. doi:10.1016/j.pain.2012.04.017

Russo AF. 2017. Overview of neuropeptides: awakening the senses? *Headache* **57**:37. doi:10.1111/HEAD.13084

Salmon AM, Damaj I, Sekine S, Picciotto MR, Marubio L, Changeux JP. 1999. Modulation of morphine analgesia in alphaCGRP mutant mice. *Neuroreport* **10**:849–854. doi:10.1097/00001756-199903170-00033

Salmon AM, Damaj MI, Marubio LM, Epping-Jordan MP, Merlo-Pich E, Changeux JP. 2001. Altered neuroadaptation in opiate dependence and neurogenic inflammatory nociception in αCGRP-deficient mice. *Nature Neuroscience 2001 4:4* **4**:357–358. doi:10.1038/86001

Scherrer G, Low SA, Wang X, Zhang J, Yamanaka H, Urban R, Solorzano C, Harper B, Hnaskod TS, Edwards RH, Basbaum AI. 2010. VGLUT2 expression in primary afferent neurons is essential for normal

acute pain and injury-induced heat hypersensitivity. *Proc Natl Acad Sci U S A* **107**. doi:10.1073/pnas.1013413108

Sharma N, Flaherty K, Lezgiyeva K, Wagner DE, Klein AM, Ginty DD. 2020. The emergence of transcriptional identity in somatosensory neurons. *Nature 2020 577:7790* **577**:392–398. doi:10.1038/s41586-019-1900-1

Sun L, Liu R, Guo F, Wen M qing, Ma X lin, Li K yuan, Sun H, Xu C lin, Li Y yuan, Wu M yin, Zhu Z gang, Li Xin jian, Yu Y qin, Chen Z, Li Xiang yao, Duan S. 2020. Parabrachial nucleus circuit governs neuropathic pain-like behavior. *Nat Commun* **11**:1–21. doi:10.1038/s41467-020-19767-w

Tso AR, Goadsby PJ. 2017. Anti-CGRP Monoclonal Antibodies: the Next Era of Migraine Prevention? *Curr Treat Options Neurol* **19**:27. doi:10.1007/s11940-017-0463-4

Vandewauw I, De Clercq K, Mulier M, Held K, Pinto S, Van Ranst N, Segal A, Voet T, Vennekens R, Zimmermann K, Vriens J, Voets T. 2018. A TRP channel trio mediates acute noxious heat sensing. *Nature* **555**:662–666. doi:10.1038/nature26137

von Euler US, Gaddum JH. 1931. An unidentified depressor substance in certain tissue extracts. *J Physiol* **72**:74–87. doi:10.1113/JPHYSIOL.1931.SP002763

Warr DG, Hesketh PJ, Gralla RJ, Muss HB, Herrstedt J, Eisenberg PD, Raftopoulos H, Grunberg SM, Gabriel M, Rodgers A, Bohidar N, Klinger G, Hustad CM, Horgan KJ, Skobieranda F. 2005. Efficacy and tolerability of aprepitant for the prevention of chemotherapy-induced nausea and vomiting in patients with breast cancer after moderately emetogenic chemotherapy. *Journal of Clinical Oncology* **23**:2822–2830. doi:10.1200/JCO.2005.09.050

Wilhelms DB, Dock H, Brito HO, Pettersson E, Stojakovic A, Zajdel J, Engblom D, Theodorsson E, Hammar ML, Spetz Holm ACE. 2018. CGRP Is Critical for Hot Flushes in Ovariectomized Mice. *Front Pharmacol* **9**. doi:10.3389/FPHAR.2018.01452

Woolf CJ, Mannion RJ, Neumann S. 1998. Null mutations lacking substance: Elucidating pain mechanisms by genetic pharmacology. *Neuron*. doi:10.1016/S0896-6273(00)80487-0

Wu Y, Luna MJ, Bonilla LS, Ryba NJP, Pickel JM. 2018. Characterization of knockin mice at the Rosa26, Tac1 and Plekhg1 loci generated by homologous recombination in oocytes. *PLoS One* **13**:e0193129. doi:10.1371/JOURNAL.PONE.0193129

Yaksh TL, Jessell TM, Gamse R, Mudge AW, Leeman SE. 1980. Intrathecal morphine inhibits substance P release from mammalian spinal cord in vivo. *Nature* **286**:155–157. doi:10.1038/286155a0

Yang D, Jacobson A, Meerschaert KA, Sifakis JJ, Wu M, Chen X, Yang T, Zhou Y, Anekal PV, Rucker RA, Sharma D, Sontheimer-Phelps A, Wu GS, Deng L, Anderson MD, Choi S, Neel D, Lee N, Kasper DL, Jabri B, Huh JR, Johansson M, Thiagarajah JR, Riesenfeld SJ, Chiu IM. 2022. Nociceptor neurons direct goblet cells via a CGRP-RAMP1 axis to drive mucus production and gut barrier protection. *Cell* **185**:4190-4205.e25. doi:10.1016/J.CELL.2022.09.024/ATTACHMENT/4531EC32-46F5-476B-BC42-F51A645ECAB6/MMC6.XLSX

Zajdel J, Sköld J, Jaarola M, Singh AK, Engblom D. 2021. Calcitonin gene related peptide α is dispensable for many danger-related motivational responses. *Scientific Reports 2021 11:1* **11**:1–9. doi:10.1038/s41598-021-95670-8

Zeisel A, Hochgerner H, Lönnerberg P, Johnsson A, Memic F, van der Zwan J, Häring M, Braun E, Borm LE, La Manno G, Codeluppi S, Furlan A, Lee K, Skene N, Harris KD, Hjerling-Leffler J, Arenas E, Ernfors P, Marklund U, Linnarsson S. 2018. Molecular Architecture of the Mouse Nervous System. *Cell* **174**:999-1014.e22. doi:10.1016/j.cell.2018.06.021

Zieglgänsberger W. 2019. Substance P and pain chronicity. *Cell Tissue Res*. doi:10.1007/s00441-018-2922-y

Zimmer A, Zimmer AM, Baffi J, Usdin T, Reynolds K, König M, Palkovits M, Mezey E. 1998. Hypoalgesia in mice with a targeted deletion of the tachykinin 1 gene. *Proc Natl Acad Sci U S A* **95**. doi:10.1073/pnas.95.5.2630